

## Climate Change and Agriculture Research Paper

**Cite this article:** Wang ZG *et al.* (2021). Study on the monitoring and classification of winter wheat freezing injury in spring based on 3S technology. *The Journal of Agricultural Science* **159**, 623–635. <https://doi.org/10.1017/S0021859621001076>

Received: 27 January 2021  
Revised: 24 December 2021  
Accepted: 30 December 2021


### Keywords:

Change vector analysis; geostatistical analysis; HuanJing-1A/1B satellite images; normalized difference vegetation index

### Author for correspondence:

M. C. Feng,  
E-mail: [fmc101@163.com](mailto:fmc101@163.com)

# Study on the monitoring and classification of winter wheat freezing injury in spring based on 3S technology

Z. G. Wang<sup>1</sup> , H. Q. Wang<sup>1</sup>, M. C. Feng<sup>1</sup>, M. X. Qin<sup>2</sup>, X. R. Zhang<sup>1</sup>, Y. K. Xie<sup>1</sup>, C. Wang<sup>1</sup>, W. D. Yang<sup>1</sup>, L. J. Xiao<sup>1</sup> and M. J. Zhang<sup>1</sup>

<sup>1</sup>Dryland Farming Engineer Institute, Shanxi Agricultural University, Taigu 030801, China and <sup>2</sup>College of Resources and Environment, Shanxi Agricultural University, Taigu 030801, China

### Abstract

Frequent freezing injury greatly influences winter wheat production; thus, effective prevention and a command of agricultural production are vital. The freezing injury monitoring method integrated with '3S' (geographic information systems (GIS), global positioning system (GPS) and remote sensing (RS)) technology has an unparalleled advantage. Using HuanJing (HJ)-1A/1B satellite images of a winter wheat field in Shanxi Province, China plus a field survey, crop types and winter wheat planting area were identified through repeated visual interpretations of image information and spatial analyses conducted in GIS. Six vegetation indices were extracted from processed HJ-1A/1B satellite images to determine whether the winter wheat suffered from freezing injury and its degree of severity and recovery, using change vector analysis (CVA), the freeze injury representative vegetation index and the combination of the two methods, respectively. Accuracy of the freezing damage classification results was verified by determining the impact of freezing damage on yield and quantitative analysis. The CVA and the change of normalized difference vegetation index ( $\Delta$ NDVI) monitoring results were different so a comprehensive analysis of the combination of CVA and  $\Delta$ NDVI was performed. The area with serious freezing injury covered 0.9% of the total study area, followed by the area of no freezing injury (3.5%), moderate freezing injury (10.2%) and light freezing injury (85.4%). Of the moderate and serious freezing injury areas, 0.2% did not recover; 1.2% of the no freezing injury and light freezing injury areas showed optimal recovery, 15.6% of the light freezing injury and moderate freezing injury areas showed poor recovery, and the remaining areas exhibited general recovery.

### Introduction

As an important food crop, wheat is mostly distributed in the temperate climate region of the Northern Hemisphere (Wang *et al.*, 2012). With the gradual warming of the global climate, freezing injury has become the main disaster occurring in the winter wheat region of northern China. When serious freezing damage occurs, it leads to significant losses in crop yield and quality (Frederiks *et al.*, 2015; Crimp *et al.*, 2016). Therefore, it is of great importance to quickly and accurately determine the severity and distribution of freezing injuries and take active and effective measures to prevent freezing injury. The traditional monitoring and evaluation methods of freezing injury of winter wheat involve measuring the lowest temperature through field observation points or meteorological stations; these methods are complicated and have certain limitations (Feng *et al.*, 2009). With the development of remote sensing (RS) technology, all kinds of multiphase, multiresolution, multispectral satellite RS systems bring the advantages of wide monitoring ranges, fast information updates, low costs, objectivity and accuracy, and unlimited study locations; thus, these methods perform better than traditional monitoring methods. With the development of geographic information systems (GIS), crop growth monitoring has developed through the use of RS data by combining global positioning system (GPS) and GIS products. Dong *et al.* (2012) evaluated the degree of winter wheat freezing injury with the freezing injury index and found that the change of normalized difference vegetation index ( $\Delta$ NDVI) had a great linear correlation with the freezing injury index and could effectively be used to evaluate the scope of influence and the degree of the disaster of winter wheat freezing injury. Wang *et al.* (2014) proposed a 'gray' system model, i.e. one designed to cope with uncertainty in a system, to evaluate the severity of winter wheat freezing injury and monitored the degree and distribution of winter wheat freezing injury with RS and GIS. Kuang *et al.* (2009) used the normalized difference vegetation index (NDVI) product of the Moderate Resolution Imaging Spectroradiometer (MODIS-NDVI) to monitor the spatial distribution and the disaster area of sugarcane freezing injury; the error in the disaster area calculation was <5%. Wang *et al.* (2005) established a

dynamic monitoring early warning system for agricultural meteorological disasters by combining '3S' (geographic information systems (GIS), global positioning system (GPS), and remote sensing (RS)) technology and ground monitoring. Some researchers have performed extensive research on the RS monitoring of winter wheat freezing injury (Yang, Wang and Pei, 2002; Feng *et al.*, 2009; Wang *et al.*, 2014), mainly by using land surface temperature (LST) inversions to calculate the occurrence level and degree of freezing injury (Gupta *et al.*, 1997).

However, the occurrence and severity of freezing injury are not only related to temperature but are also affected by plant varieties, irrigation conditions, and other factors. NDVI has a significant correlation with the growth and yield of winter wheat. The change in NDVI could be reasonably used to represent the severity of a freezing injury (Zhao *et al.*, 2020). With the aggravation of freezing injury, the red-edge region of the reflectance of a winter wheat canopy increases, the green region reflectance decreases, and the red-edge position obviously moves towards the blue band; this is called a 'blueshift' (Ren *et al.*, 2014). This change in spectral reflectance makes it possible to monitor the freezing injury of winter wheat by RS. The NDVI values of winter wheat decrease significantly with the blueshift phenomenon. Certain researchers have used NDVI values obtained from RS data to evaluate the degree of winter wheat freezing injury (Kerdiles *et al.*, 1996; Feng *et al.*, 2009; Wang *et al.*, 2013). Remotely sensed vegetation indexes such as NDVI and enhanced vegetation index (EVI) are regarded as reliable indicators for estimating productivity and monitoring vegetation conditions globally (Myneni and Williams, 1994; Cuomo *et al.*, 2001; Lanfredi, 2003; Bascietto *et al.*, 2012). Therefore, the change in the NDVI was used to monitor the occurrence (Jurgens, 1997) and spatial distribution of Tan *et al.* (2008) and to assess the damage caused by freezing crops (Tan *et al.*, 2008; Feng and Yang, 2010).

Since temperature is not the only factor affecting freezing injury,  $\Delta$ NDVI tends to overestimate the coverage rate of winter wheat before ridge sealing. Many researchers have studied the change vector analysis (CVA) method to estimate the freezing injury of winter wheat. In the CVA method, the change direction and amplitude are obtained by comparing two feature vectors of different time courses (Zhu, 2017). By processing satellite images in different stages, this method can avoid unreasonable classification defects caused by accumulated errors (Zhu, 2017). This method can also reflect the degree and spatial distribution of winter wheat freezing injury and growth recovery and provide a foundation for the monitoring of other crop disasters (Wang *et al.*, 2011). The CVA method has a strong application in dynamic monitoring. Sun *et al.* (2015) found that a combination of map points and CVA can make full use of object-oriented sample land information and can extract crops more accurately on the basis of crop change information when supplemented by a standardized vegetation index. Through a change vector sensitivity analysis, Zhu (2017) found a great correlation between the total erosion of wheat and the enhancement of the vegetation index.

These two approaches (CVA and  $\Delta$ NDVI) have been useful for monitoring crop freezing injury and in addition have different characteristics and emphases. Thus far, both approaches have been used independently. The aim of the current study was to study the effects of the freezing injury degree and the recovery degree on winter wheat yield, and to explore a more accurate monitoring method, using a combination of CVA and  $\Delta$ NDVI to monitor freezing injury in winter wheat. According to the statistical analysis, spatial distribution maps of the degree of freezing

injury, recovery rate and winter wheat yield were obtained to monitor the freezing injury of winter wheat; these results will provide the scientific basis for the monitoring of winter wheat freezing injury and the evaluation of crop production.

## Materials and methods

### Sampling and data collection

Thirty-four winter wheat fields were selected from the study areas of Wenxi County, Shanxi Province, China (35°9'–35°34' N, 110°59'–111°37' E, 450–1500 m a.s.l.) in 2010; each wheat field had a size of at least 5 ha. At the mature wheat stage, the yield components (spike number, grain number per spike, thousand-grain weight) were investigated to determine the yield. Specifically, in each plot, 1 m × 1 m of above-ground plants was harvested manually and brought to the lab for processing. Triplicate plots (50 m × 50 m) were sampled in each field. Abnormal wheat yield values were eliminated by SPSS 20.0 software.

A GPS product (Brand: Jiaming, Model: G120BD, country of origin: China) was used in the study region for accurate positioning. ENVI 5.0 was used to process the RS images obtained from the HuanJing (HJ)-1A/1B satellite charge coupled device (CCD). ArcGIS 10.0 was used to process the related GIS content. SPSS 20.0 was used for various data analyses described in the text.

### Preprocessing of the HuanJing-1A/1B satellite charge coupled device data

The HJ-1A/1B CCD data, whose spatial resolution was 30 m × 30 m, were provided by the China Centre for Resources Satellite Data and Application. In the present study, the HJ1A-CCD1-8-72-20100223 data set was used to extract the winter wheat planting area, and the HJ1B-CCD2-7-71-20100410, HJ1B-CCD1-6-72-20100424 and HJ1B-CCD1-9-71-20100510 data sets were used to extract the vegetation indexes. The ratio vegetation index, difference vegetation index, NDVI, EVI, structure insensitive pigment index (SIPI) and green ratio vegetation index were adopted as six-dimensional spatial vectors.

### Pretreatment method

**Atmospheric correction:** The Fast Line-of-sight Atmospheric Analysis of Spectral Hypercubes (FLAASH) module was used to adjust the HJ-1A/1B RS images.

**Geometric correction:** A coarse geometric-correction and precise geometric-correction process were completed using a 1:50 000 digital raster map and ground control points. A cubic convolution interpolation was used to assure that the error was less than one pixel in the georeferencing process (Chen, 2012).

**Calculation of VI:** The vegetation indices (VIs) of the HJ-1A/1B images were calculated using the following methods (Table 1).

**Extraction of planting area:** First, an atmospheric correction was performed on the HJ-1A data, and ground control points were used for the geometric correction. The Mahalanobis distance taxonomy was used to classify the data, and the classification effect was the best when the threshold was set to 2.9. To address the leakage and spillage fractions remaining in the images after classification, each planting area vector graph produced by classification was superimposed with the corresponding HJ-1A RS image in ArcGIS through a second visual interpretation to ultimately produce an area vector graph. An HJ-1A image of the winter

**Table 1.** The introduction of six vegetation indexes

Vegetation index	Formula	References
RVI	$R_{NIR}/R_{RED}$	Anderson <i>et al.</i> (1993)
DVI	$R_{NIR} - R_{RED}$	Richardson and Wiegand (1977)
NDVI	$(R_{NIR} - R_{RED})/(R_{NIR} + R_{RED})$	Rouse <i>et al.</i> (1974)
EVI	$2 \times (R_{NIR} - R_{RED}) / (R_{NIR} + 6 \times R_{RED} + 7.5 \times R_{BLUE} + 1)$	Liu and Huete (1995)
GRVI	$R_{NIR}/R_{GREEN} - 1$	Gitelson <i>et al.</i> (1996)
SIPI	$(R_{NIR} - R_{BLUE}) / (R_{NIR} - R_{RED})$	Penuelas <i>et al.</i> (1995)

RVI, ratio vegetation index; DVI, difference vegetation index; NDVI, normalized difference vegetation index; EVI, enhanced vegetation index; GRVI, green ratio vegetation index; SIPI, structure insensitive pigment index.  $R_{NIR}$  is reflectance of near infrared band;  $R_{RED}$  is reflectance of red band;  $R_{BLUE}$  is reflectance of blue band;  $R_{GREEN}$  is reflectance of green band.

wheat planting area was obtained by cutting the HJ-1A image in ENVI (Fig. 1).

### Construction of the change vector

The six-dimensional spatial vector was constructed from the six vegetation indexes described above, and each pixel on the three-stage images corresponded to a six-dimensional vegetation index vector, as follows:

$$P_{ij} = [t_1, t_2, t_3, t_4, t_5, t_6]^T \tag{1}$$

In the formula,  $t$  is the six-vegetation index;  $i$  is the phase image, where  $i = 1, 2, 3$ ; and  $j$  is the pixel on a phase image. The module length and directional cosine were calculated as shown in Eqn (2):

$$|P_{ij}| = \sqrt{t_1^2 + t_2^2 + t_3^2 + t_4^2 + t_5^2 + t_6^2} \tag{2}$$

$$\cos \theta = \frac{t_n}{|P_{ij}|}, \quad n = 1, 2, 3, 4, 5, 6 \tag{3}$$

According to the spatial vector constructed using the six vegetation indexes described above, the spatial angle vector of each pixel is obtained, and the angle change vector in space is constructed as follows:

$$\Delta\theta_1 = \begin{Bmatrix} \theta_{2,j,1} - \theta_{1,j,1} \\ \theta_{2,j,2} - \theta_{1,j,2} \\ \theta_{2,j,3} - \theta_{1,j,3} \\ \theta_{2,j,4} - \theta_{1,j,4} \\ \theta_{2,j,5} - \theta_{1,j,5} \\ \theta_{2,j,6} - \theta_{1,j,6} \end{Bmatrix}, \quad \Delta\theta_2 = \begin{Bmatrix} \theta_{3,j,1} - \theta_{2,j,1} \\ \theta_{3,j,2} - \theta_{2,j,2} \\ \theta_{3,j,3} - \theta_{2,j,3} \\ \theta_{3,j,4} - \theta_{2,j,4} \\ \theta_{3,j,5} - \theta_{2,j,5} \\ \theta_{3,j,6} - \theta_{2,j,6} \end{Bmatrix} \tag{4}$$

$\Delta\theta_1$  reflects whether winter wheat has suffered from freezing injury and the severity of the freezing injury and  $\Delta\theta_2$  reflects the degree of winter wheat growth recovery following freezing injury. The vegetation index with the largest change range was selected as the best index for use in freezing injury monitoring applications because the larger the change range is, the more obvious the change degree of pixels is.

### Monitoring of the freezing injury of winter wheat by the change of normalized difference vegetation index

The NDVI values obtained in each neighbouring stage were used to monitor freezing injury. That is,  $\Delta NDVI_1 = NDVI_2 - NDVI_1$ . In this formula,  $NDVI_1$  is the NDVI value recorded before the occurrence of a freezing injury, and  $NDVI_2$  is the NDVI value obtained during the freezing injury period. If  $\Delta NDVI_1 > 0$ , winter wheat is not affected by freezing injury; if  $\Delta NDVI_1 = 0$ , the growth of winter wheat is suppressed; and if  $\Delta NDVI_1 < 0$ , winter wheat is affected by freezing injury.

The NDVI values obtained before and after freezing injury were used to monitor the degree of growth recovery following freezing injury. That is,  $\Delta NDVI_2 = NDVI_3 - NDVI_1$ , in which  $NDVI_1$  is the NDVI value measured before the occurrence of freezing injury and  $NDVI_3$  is the NDVI value recorded after the freezing injury period.

### Geostatistical analysis

Through the analyses, it was ensured that the relevant data were normally distributed, and the kriging interpolation method (Huang *et al.*, 2015; Cao *et al.*, 2018) was used to obtain the spatial distributions of the analysed data.

### Results and analysis

#### Monitoring of winter wheat based on the change vector analysis results

According to Eqns (3) and (4), the spatial vector angle ranges of the six considered vegetation indexes can be obtained for all pixel characterizations. The ranges of  $\Delta\theta_1$  and  $\Delta\theta_2$  are shown in Table 2. The range in  $\Delta\theta$  ( $j$ , NDVI) is the largest, so NDVI is used to characterize the winter wheat freezing injury and recovery degrees (Table 2).

The freezing injury degree can be divided into four grades according to the range in  $\Delta\theta_1$  ( $j$ , NDVI) and the change in the winter wheat yield following the freezing injury; this range can indicate normal ( $-12.00^\circ, -4.45^\circ$ ), light ( $-4.45^\circ, 6.62^\circ$ ), moderate ( $6.62^\circ, 13.45^\circ$ ) and serious ( $13.45^\circ, 21.85^\circ$ ) freezing injury degrees. Small portions of the northeast and southwest regions of the studied county suffered serious freeze-related damage, and some moderate freezing injury occurred around the wheat-growing areas that suffered from serious freezing injury (Fig. 2(a)). A small part of the freezing injury areas was not affected, and most areas suffered only a slight freezing injury.

The recovery degree of winter wheat following a freezing injury can be divided into four grades according to the range in  $\Delta\theta_2$  ( $j$ , NDVI) and according to the actual investigation results: these grades include not recovered ( $-13.48^\circ, -5.00^\circ$ ), poorly recovered ( $-5.00^\circ, 2.00^\circ$ ), generally recovered ( $2.00^\circ, 14.00^\circ$ ) and optimally recovered ( $14.00^\circ, 22.35^\circ$ ). There were few areas without freezing injury in Wenxi County, and other areas suffered from different degrees of freezing injury (Figs 2(a) and (b)). A small part of the central region suffered serious freezing injury, and a small part of this region did not recover; the recovery of winter wheat growth was poor in the eastern part of the central region, which suffered moderate freezing injury; the degree of recovery was general in most of the region in which the freezing injury was light; and in the small region where no freezing injury occurred, the degree of recovery was general (Figs 2(a) and (b)).

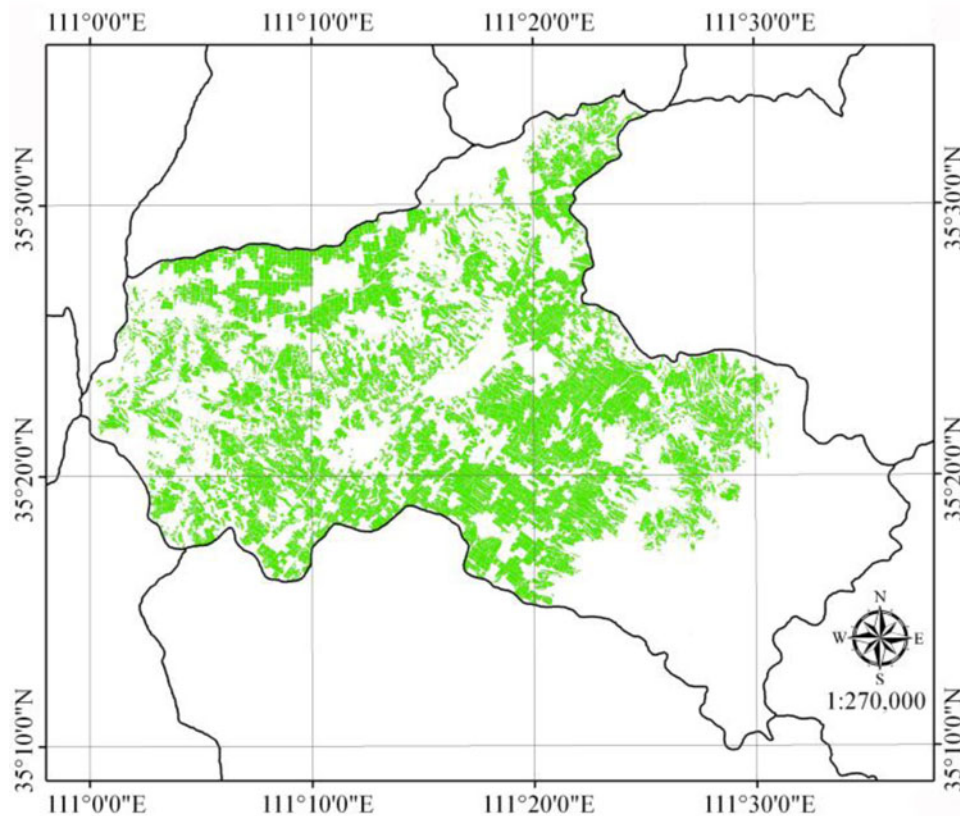


**Fig. 1.** Colour online. Extraction of planting area of winter wheat in Wenxi County, Shanxi Province, China in 2010.

**Table 2.** Range of special vector angle about vegetation indexes

Angle change phase	Change range	$\Delta\theta_{(j, DVI)}$	$\Delta\theta_{(j, RVI)}$	$\Delta\theta_{(j, NDVI)}$	$\Delta\theta_{(j, EVI)}$	$\Delta\theta_{(j, GRVI)}$	$\Delta\theta_{(j, SIPI)}$
$\Delta\theta_1$	Min	-12.60°	-4.72°	-12.00°	-11.05°	-10.16°	-16.75°
	Max	10.90°	2.72°	21.83°	13.19°	8.32°	12.78°
$\Delta\theta_2$	Min	0.15°	-0.85°	-13.48°	-19.74°	-11.40°	-4.03°
	Max	-24.10°	5.76°	22.35°	12.45°	2.88°	20.24°

DVI, difference vegetation index; RVI, ratio vegetation index; NDVI, normalized difference vegetation index; EVI, enhanced vegetation index; GRVI, green ratio vegetation index; SIPI, structure insensitive pigment index;  $\Delta\theta_1$  and  $\Delta\theta_2$  were the angle change vectors in space,  $\Delta\theta$  reflects whether winter wheat has suffered from freezing injury and the severity of the freezing injury and  $\Delta\theta_2$  reflects the degree of winter wheat growth recovery following freezing injury.

### Monitoring of winter wheat based on the change of normalized difference vegetation index

In the process by which the winter wheat freezing injury is monitored based on a CVA, the range in  $\Delta\theta(j, NDVI)$  was the largest, indicating a significant change in pixels following the freezing injury of winter wheat. Therefore, it was necessary to analyse the effect of winter wheat freezing injury on NDVI variability.

The NDVI value suddenly drops following a freezing injury of winter wheat. According to the change in the winter wheat NDVI recorded before and after a low-temperature event, it can be determined whether the winter wheat was affected by a freezing injury. When  $\Delta NDVI_1 > 0$ , winter wheat has not been affected by a freezing injury. When  $\Delta NDVI_1 \leq 0$ , winter wheat has been affected by a freezing injury, and the smaller the  $\Delta NDVI_1$  value is, the greater the effect of the freezing injury was. It can be seen from the spatial distribution of  $\Delta NDVI$  (Fig. 3(a)) that very small parts of the

northeast and southwest regions suffered from serious freezing injury. Some moderate freezing injury occurred around the wheat-planting area that suffered from serious freezing injury. A small portion of the area was not affected; most areas suffered freezing injury at only a light degree.

With the end of a freezing injury, the temperature gradually increases, winter wheat begins to resume its growth, and the NDVI values also gradually increase. However, because of the differences in the freezing injury temperatures and durations among different areas, the degree of winter wheat freezing injury is also different, and the speed and degree of its recovery are thus different. Therefore, the NDVI difference recorded before and after a freezing injury could be used to monitor the growth recovery degree of winter wheat following a freezing injury. When  $\Delta NDVI_2 > 0$ , it indicates that winter wheat has recovered its growth; the larger the  $\Delta NDVI_2$  value is, the greater the degree

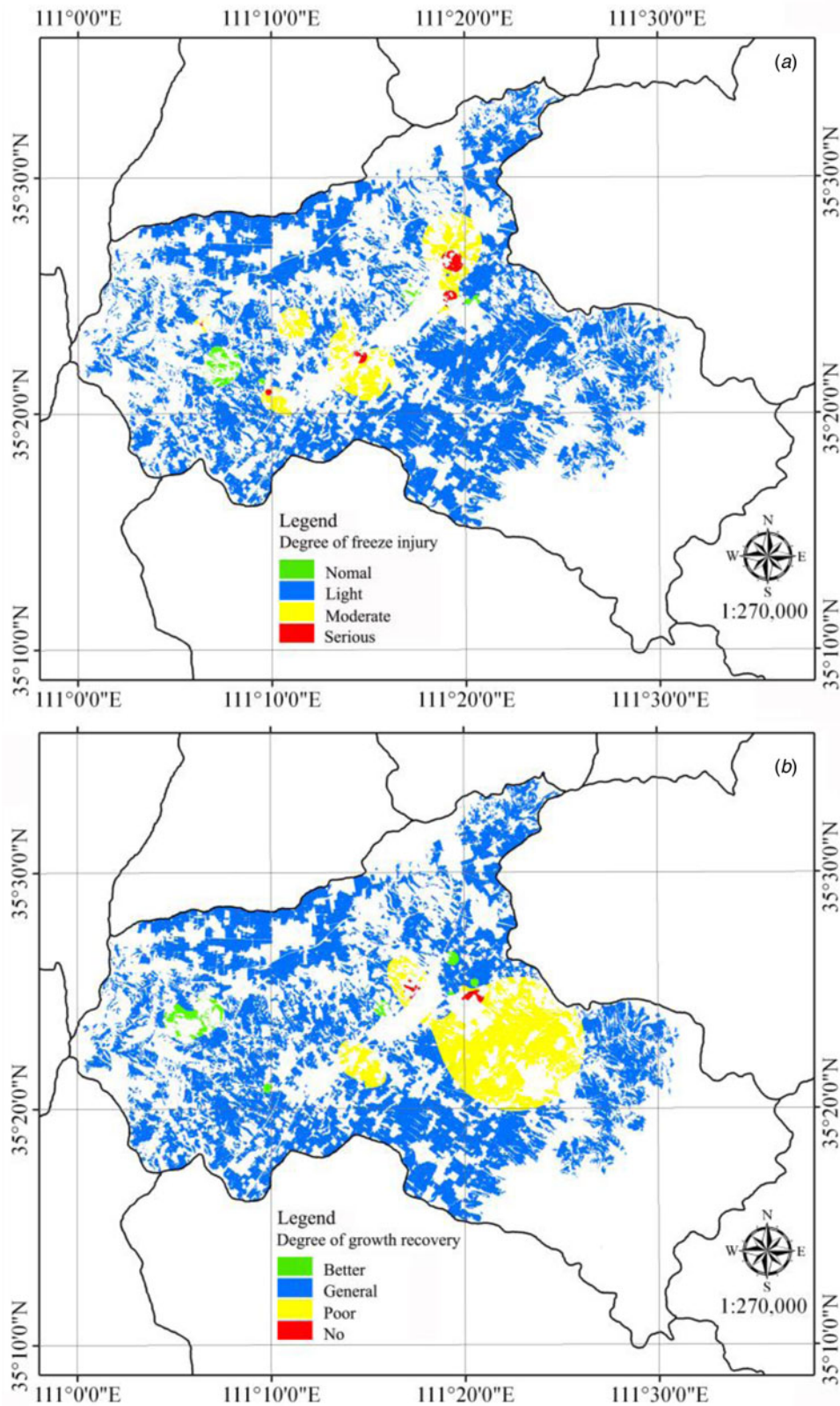


**Fig. 2.** Colour online. Spatial distribution image of  $\Delta\theta_1(j, NDVI)$  and  $\Delta\theta_2(j, NDVI)$ .  $\Delta NDVI$ , the change of normalized difference vegetation index;  $NDVI$ , normalized difference vegetation index;  $\Delta\theta_1(j, NDVI)$  and  $\Delta\theta_2(j, NDVI)$  was the angle change vector in space.  $\Delta\theta_1(j, NDVI)$  reflects whether winter wheat has suffered from freezing injury and the severity of the freezing injury and  $\Delta\theta_2(j, NDVI)$  reflects the degree of winter wheat growth recovery following freezing injury.

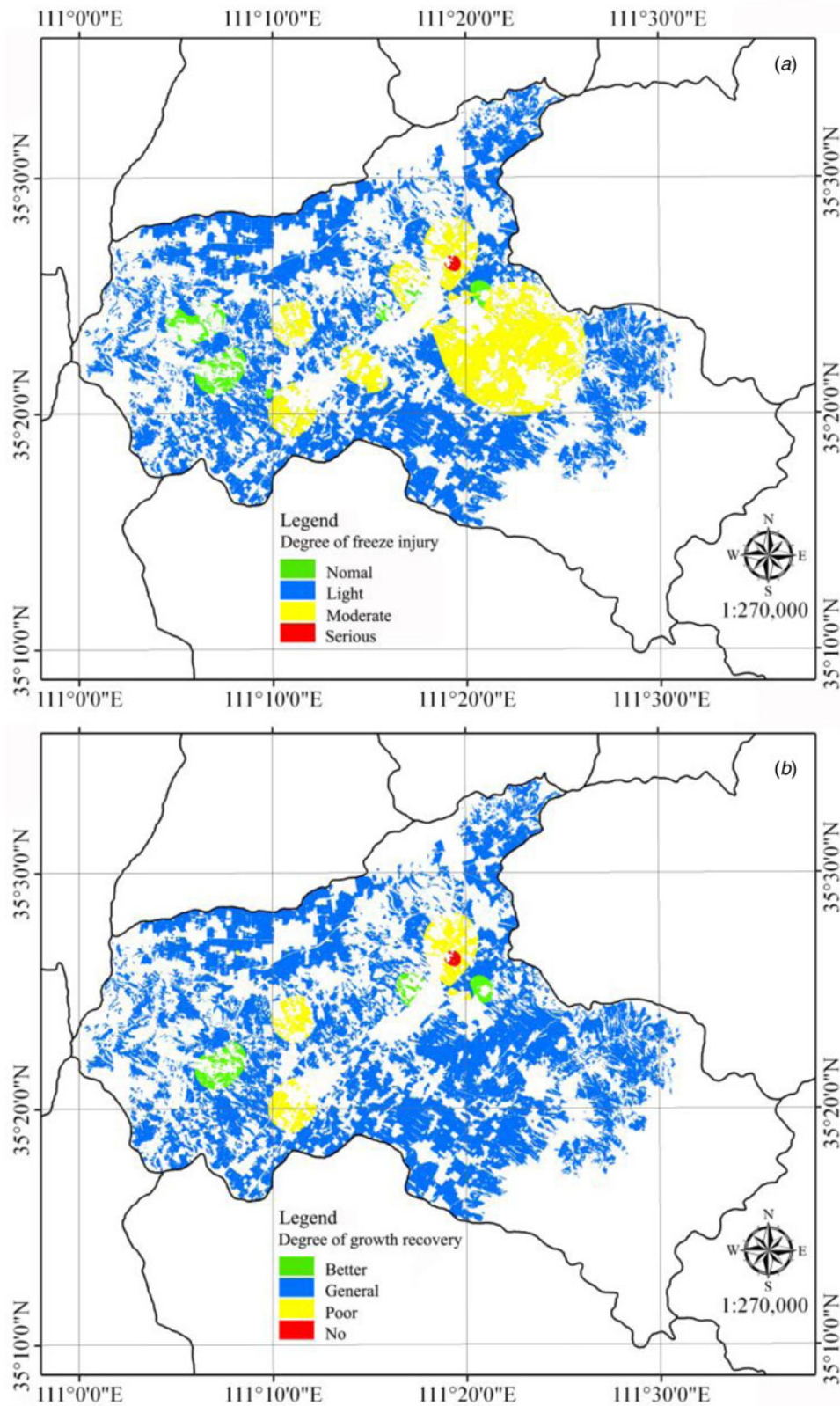


**Fig. 3.** Colour online. Spatial distribution image of  $\Delta\text{NDVI}_1$  and  $\Delta\text{NDVI}_2$ .  $\Delta\text{NDVI}$ , the change of normalized difference vegetation index;  $\Delta\text{NDVI}_1 = \text{NDVI}_2 - \text{NDVI}_1$ . In this formula,  $\text{NDVI}_1$  is the NDVI value recorded before the occurrence of a freezing injury, and  $\text{NDVI}_2$  is the NDVI value obtained during the freezing injury period,  $\Delta\text{NDVI}_2 = \text{NDVI}_3 - \text{NDVI}_1$ , in which  $\text{NDVI}_1$  is the NDVI value measured before the occurrence of freezing injury and  $\text{NDVI}_3$  is the NDVI value recorded after the freezing injury period.

of recovery is. When  $\Delta\text{NDVI}_2 \leq 0$ , it indicates that the internal structure of the winter wheat has changed, and it cannot recover its growth. From the spatial distribution of  $\Delta\text{NDVI}_2$  (Fig. 3(b)), a small unrecovered area can be seen throughout the whole county, and the recovery was poor in the areas surrounding this region; most of the studied areas underwent optimal recovery.

The winter wheat in the area that suffered serious freezing injury had not yet recovered at the time of analysis (Fig. 3). The region that suffered moderate freezing injury generally had a poor recovery or even no recovery, and the area that was not affected by freezing injury had a general or optimal recovery (Fig. 3).

### Comprehensive monitoring of winter wheat freezing injury

The CVA and  $\Delta\text{NDVI}$  results were roughly the same, but there were also some differences. It was necessary to combine these two methods into a comprehensive analysis to obtain more accurate monitoring results.

### Comprehensive monitoring of the freezing damage of winter wheat

The locations of the areas indicated to have suffered severe freezing injury by the two methods were exactly the same, and the areas that did not suffer from freezing injury were also generally consistent (Figs 2(a) and 3(a)). However, the areas under moderate and light freezing injury were not equal between the two methods; the freezing injury situation in the sampling area and the surrounding areas were exactly the same and appropriate, and the area of moderate freezing injury was located near the severe freezing injury area and far away from the no freezing injury area, while the remaining area suffered light freezing injury (Figs 2(a) and 3(a)). The degree of freezing damage in the figure is analysed, and it is found that there is a certain inclusive relationship between different degrees of freezing damage (Figs 2(a), 3(a) and 4).

According to the inclusive relationship of freeze injury severity (Fig. 4), the regions corresponding to the same freezing injury level were jointly processed by the superposition analysis tool of ArcGIS (Figs 2(a) and 3(a)). The area without freezing injury was considered the final area without any freezing injury, and the area with serious freezing injury was considered the final area with severe freezing injury. The final moderate freezing injury area was obtained by erasing the moderate freezing damage area with the erasing tool; then, the above three winter wheat planting areas were erased to obtain the final light freezing injury area (Fig. 5).

The spatial distribution of the freezing injury degree of winter wheat was consistent with the inclusion relationship (Fig. 4); however, the level of the regional area changed. Due to the limitations of the sampling points, the interpolation shown on the graph was most accurate at the location of the sampling point; the interpolation results become less accurate with an increasing distance from the sampling area. However, the severe freezing injury and no freezing injury areas were small, and there were sampling points in these ranges, so these results could be approximately considered as accurate. The moderate injury union area covered a small portion of the serious injury union area, so this area had to be erased. The rest of the studied region comprised light-injury areas. There was no sampling point at the border area of Wenxi County, and the interpolation results were not accurate in this region.

Statistical analysis of the area under different degrees of freezing injury showed that the area suffering serious freezing injury was the smallest proportion, accounting for 0.9% of the total

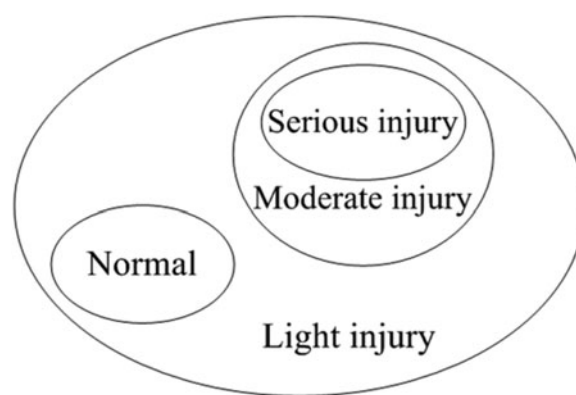


Fig. 4. Inclusive relationship between different degrees of freezing damage.

study area, followed by the area with no freezing injury, which accounted for 3.5%, and the area of moderate freezing injury, which accounted for 10.2%; the remaining area experienced light freezing injury (Table 3).

### Comprehensive monitoring of the recovery degree of winter wheat following a freezing injury

The output optimal recovery region was basically consistent between the two methods, while differences could be seen in the locations and areas of the other degrees of recovery (Figs 2(b) and 3(b)). By analysing the degree of growth recovery in the graph, the areas with poor recovery rates, including areas with no recovery, were separated from the recovered areas, and the remaining areas were considered normal recovery areas (Figs 2(b) and 3(b)). Thus, the inclusive relationship between different degrees of growth recovery can be obtained (Fig. 6).

To comprehensively monitor the growth and recovery of winter wheat in Wenxi County, a methodical approach to comprehensively analysing the degree of freezing injury was used to divide the recovery level of the winter wheat area with the superposition analysis tool in ArcGIS. The not-recovered region obtained by  $\Delta\theta_2$  ( $j$ , NDVI) was located in the no freezing injury area (Fig. 5), which was unreasonable. Therefore, this part of the not-recovered region was discarded, and the not-recovered region obtained by  $\Delta\text{NDVI}_2$  was taken as the final recovery region. The areas of optimal recovery output by the two methods were combined to obtain the optimal recovery area, and the areas overlapping with the not-recovered region were erased to obtain the final optimal recovery area. By combining the poor-recovery areas output by the two methods, a comprehensive poor-recovery area was obtained, and the part of this region that overlapped with the optimal recovery rate area was deleted to obtain the final poor-recovery area; the rest of the study region was considered the general recovery area (Fig. 7).

The area of each level also changed due to alteration of the search radius at the time of interpolation, and the results did not conform to the inclusion relation (Figs 6 and 7). Similarly, the closer the sampling area was to the measured point, the more accurate the output recovery degree was. Because the sampling point was concentrated in a region of Wenxi County, the resulting interpolation graph was not accurate at the county boundary regions. However, the sampling points located near the boundary indicated general recovery, so the boundary region was classified as a general recovery area.

Statistical analysis of the area under different degrees of growth recovery showed that the area unable to recover was the smallest

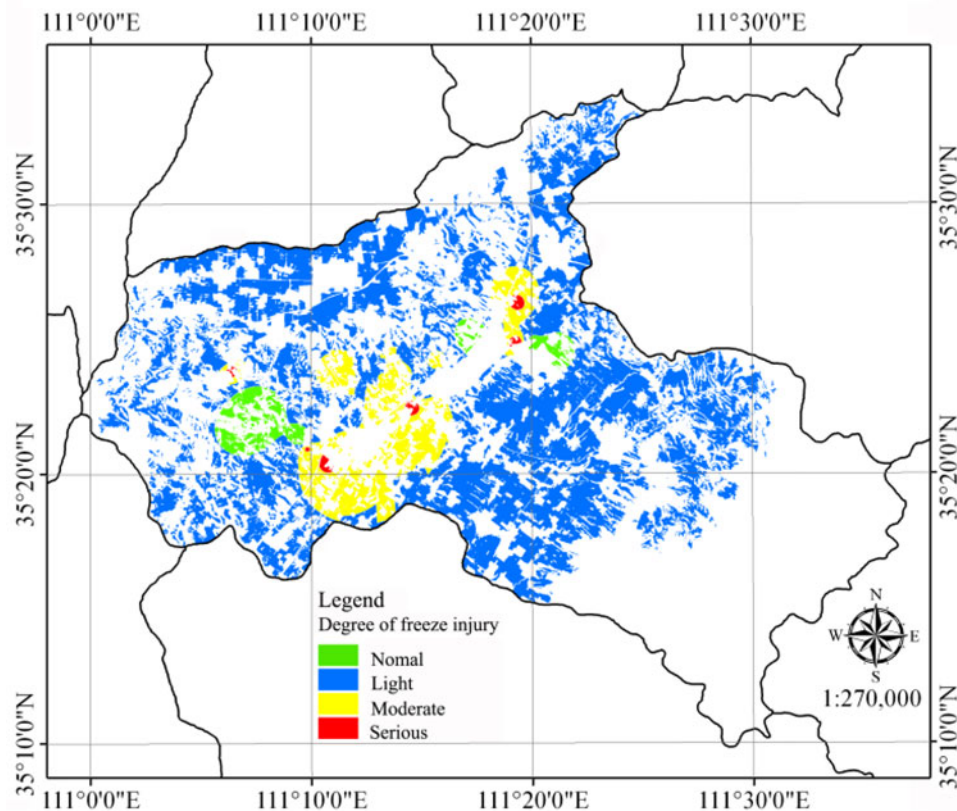


Fig. 5. Colour online. Spatial distribution image of freeze injury degree.

Table 3. Statistical analysis of the degree of freeze injury and growth recovery

Attributes	Degree	Area (ha)	Proportion (%)
Freeze injury	Serious	390	0.9
	Moderate	4457	10.2
	Light	37 458	85.4
	Normal	1529	3.5
Growth recovery	No	88	0.2
	Poor	6818	15.6
	General	36 384	83.0
	Better	544	1.2

proportion, accounting for 0.2%, followed by the well-recovered area, which accounted for 1.2%; the poorly-recovered area accounted for 15.6%, and the rest was the general recovery area (Table 3). Winter wheat that was exposed to serious freezing injury did not recover or recovered poorly and the recovery of winter wheat in the moderate freezing injury area was generally poor, while the areas not affected by freezing injury showed general or optimal recovery (Figs 5 and 7).

#### The effects of freezing injury on winter wheat yield

Different degrees of freezing injury have different effects on the winter wheat yield. According to the statistical analysis conducted herein, the distribution of the winter wheat yield in Wenxi County

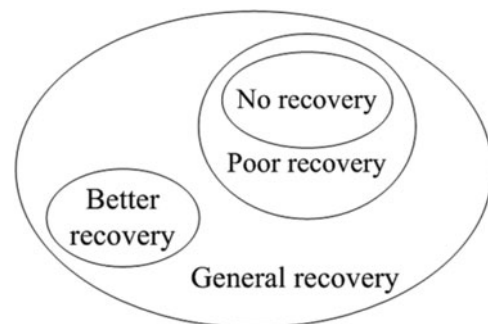


Fig. 6. Inclusive relationship between different degrees of restoring degree.

showed a normal distribution, so the yield distribution of Wenxi County was obtained by the kriging interpolation method (Fig. 8).

The winter wheat yield was highest in the area without freezing injury and the area with optimal recovery, spanning a region more than 3000 kg/ha in area. In the light freezing injury and general-recovery areas, the winter wheat yield ranged from 2601 to 3000 kg/ha; in the areas of serious and moderate freezing injury, the winter wheat yield ranged from 2331 to 2600 kg/ha; and the wheat yield was under 2330 kg/ha in the area where the recovery following freezing injury was poor (Figs 5, 7 and 8). The degree of freezing injury, the grade of recovery and the grade of yield (actual yield) are represented by I, II, III and IV (Table 4).

SPSS was used for the correlation analysis among the yield grade and the freezing injury grade and recovery grade; a regression model was constructed, and leave-one-out cross-validation



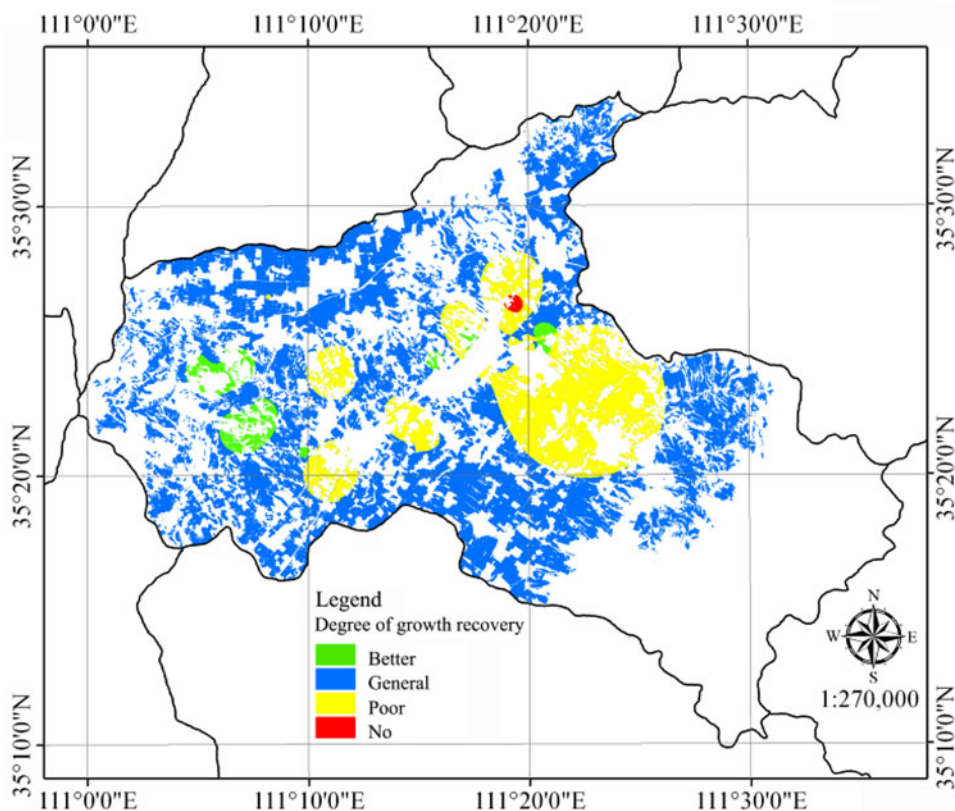


Fig. 7. Colour online. Spatial distribution image of winter wheat growth recovery rates.

was used to verify the results of the regression model. The results showed that in the regression model outputs characterizing the freezing injury grade, recovery grade and yield grade,  $R$  was 0.696 and 0.596,  $P$  was 0.001 and 0.006, respectively; the  $R$  of the verification results was 0.697 and 0.631, and  $P$  was 0.012 and 0.039, respectively (Table 5). In the regression model that predicted the yield grade using the freezing injury grade and recovery grade, the regression model had an  $R$  value of 0.771 and a  $P$  value of 0.006 (freeze injury level) and 0.045 (recovery degree level). In the verification results,  $R$  was 0.782 and  $P$  was 0.016 (Table 5). The verification results show that the regression models are relatively stable and can be used to predict the yield classification results to a large extent. In the results, the significance values of the regression coefficients of each model were  $<0.05$ , indicating that each model passed the 0.05 significance level test and that there were significant correlations among the yield level, freezing injury level and recovery level (Table 5), indicating that the freezing damage grade and recovery grade are of great significance when predicting the yield grade. Therefore, the yield level could be determined by selecting the level of freezing injury and the degree of recovery following injury to understand the measured yield range (Fig. 9).

This study judged the model prediction results based on the magnitudes of the  $R^2$  and s.e. indicators. The larger the  $R^2$  and the smaller the s.e. values were, the better the prediction effect of the model was. The  $R^2$  of the model that was jointly predicted by the level of freezing injury and the level of recovery was the largest, and the s.e. value was the smallest (Table 5). The yield range of winter wheat after freezing injury can thus be estimated more accurately using this method. Therefore, by combining the degree

of freezing injury and the degree of recovery following a freezing injury in winter wheat, the winter wheat freezing injury and the impact on yield can be simulated well. At the same time, by the division of yield grades, the accuracy of the freezing injury classification can be verified.

## Discussion

Compared with the traditional methods, the applications of RS monitoring technologies to studies of winter wheat freezing injury have made some progress, and these methods have wide scopes, are fast, save time and costs, and have other advantages, thus showing great potential. However, for a long time, research on freezing injuries was limited to surface temperature inversions, and research on freezing damage monitoring combined with ground data was limited.

It is obvious that when using the vector of change method and a single vegetation index to analyse freezing damage, the two utilized methods have roughly the same location and area differences in the freezing-damaged area (Figs 2 and 3). Regarding the division of the restoration area, the two methods differ not only in the location of recovering areas but also in the size of these areas (Figs 2(b) and 3(b)). These area differences may be related to the fact that NDVI tends to overestimate the vegetation coverage before ridge closure, while the change vector method can estimate the direction of a pixel change.

To monitor freezing damage more accurately, a comprehensive analysis method can be used to obtain the final wheat-freezing-damage information. The results of this study show that few areas in the study region have not suffered freezing

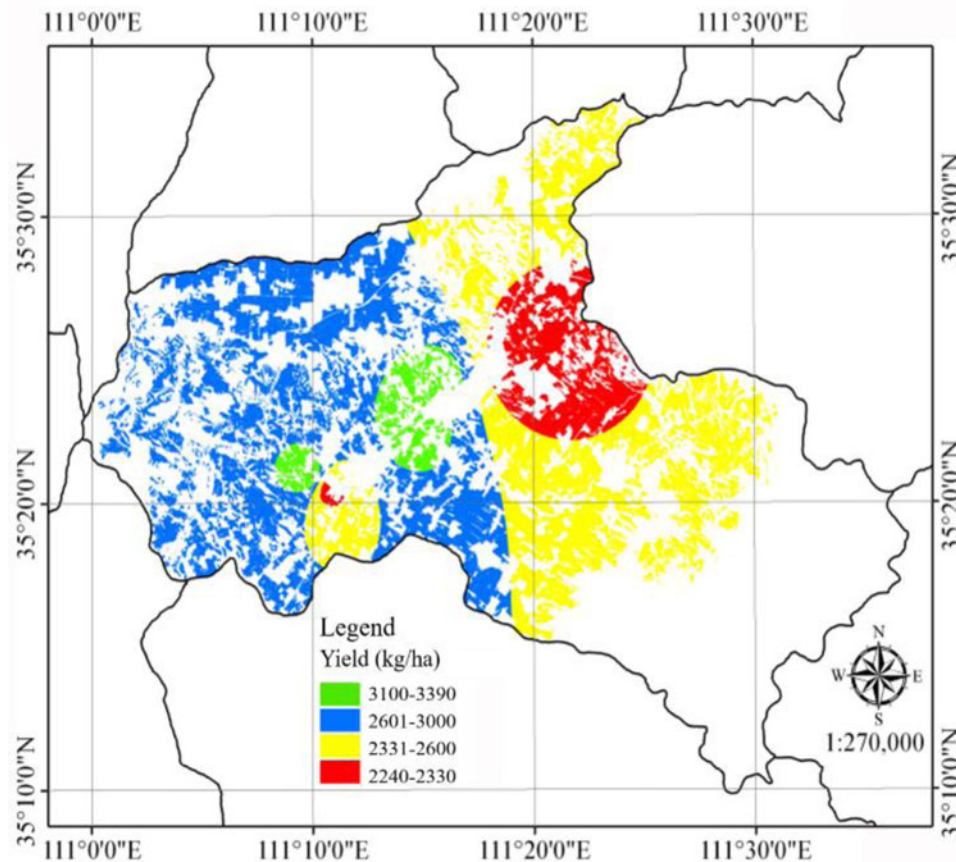


Fig. 8. Colour online. Spatial distribution image of yield of winter wheat.

Table 4. Grading of degree of freezing injury, the degree of recovery and the level of yield

Indicators	Level			
	I	II	III	IV
Degree of freeze injury	Serious	Moderate	Light	Normal
Degree of growth recovery	No	Poor	General	Better
Yield (kg/ha)	2240–2330	2331–2600	2601–3000	3100–3390

damage, while the other areas have suffered different degrees of freezing damage (Fig. 5). It is speculated that the low-temperature weather that occurred from 10 to 28 March kept the winter wheat plants in low-temperature conditions for a long time, causing the winter wheat to suffer extensive freezing damage. A very small part of the central region suffered severe freezing damage, and a small part did not resume growth following this damage. This may have been because the winter wheat plants were affected by extremely low temperatures from 12 to 15 April, causing changes in the internal structures of the winter wheat plants and resulting in irreversible changes that prevented the plants from growing and caused them to die. In the areas that suffered moderate freezing damage east of the central study area, the recovery of winter wheat growth was poor, and most of the areas with slight freezing damage also showed normal recovery (Figs 5 and 7). This result may have been caused by freezing

damage inhibiting the growth of winter wheat. The areas that were not affected by freezing showed fair or optimal recovery, indicating the normal growth of winter wheat.

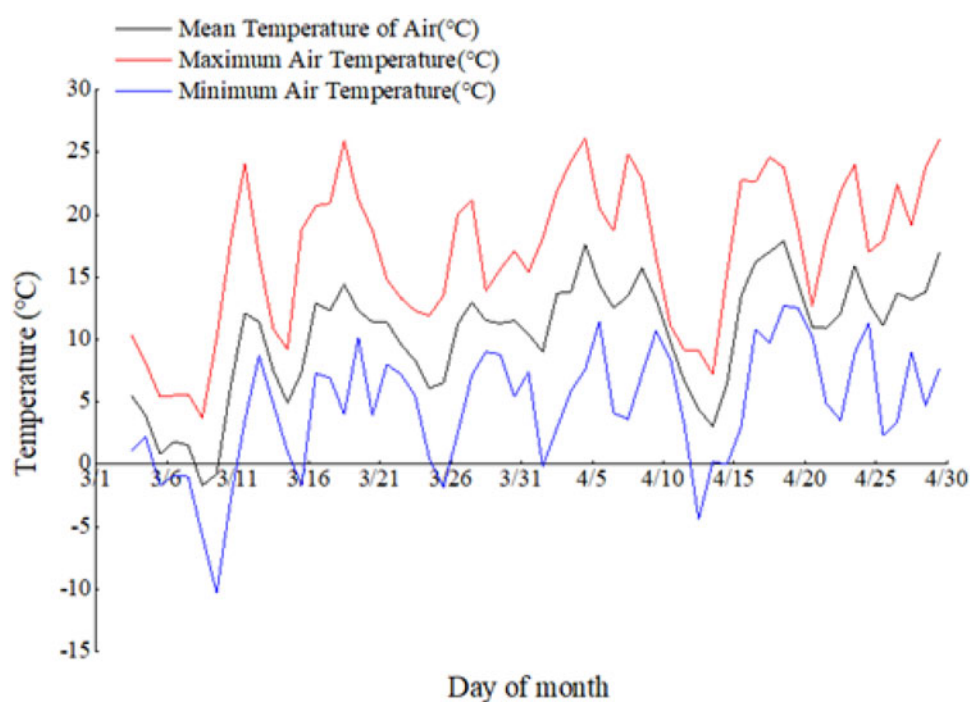
After a freezing injury, the crops began to resume growth as the temperature increased. However, because of the differences in the surface temperature and the low-temperature duration, the degree of freezing injury and the speed of growth also differed. For example, following a winter wheat freezing injury, the growth period was extended, resulting in an inconsistent mature period and inconsistent production losses.

After crops suffer from a freezing injury, their frozen tissues and organs suddenly desiccate, lose their remaining green pigment, lose water, wilt and dry up. This performance is a gradual process, so there is a certain hysteresis effect that prevents the crop injury situation from being fully reflected when monitoring crops using the vegetation index before and following a freezing injury.

**Table 5.** Prediction model of yield level ( $n = 20$ )

Independent variables	Data set	$R$	$R^2$	$P$	s.e.
Freeze injury level	Cal	0.696	0.484	0.001	0.651
	Val	0.697	0.486	0.012	
Recovery degree level	Cal	0.596	0.355	0.006	0.728
	Val	0.631	0.398	0.039	
Freeze injury/recovery degree level	Cal	0.771	0.548	0.006/0.045	0.594
	Val	0.782	0.548	0.016	

Cal, calibration; Val, validation;  $R^2$ , coefficient of determination;  $P$ , significance; s.e., standard error. Leave-one-out cross-validation was used to verify the results of the regression model.

**Fig. 9.** Colour online. Diurnal variations of air temperature in March and April 2010 in Wenxi County, Shanxi Province, China.

At the same time, this lagging performance also induces certain risks when conducting immediate disaster relief measures. However, from a macroscopic point of view, the methods utilized herein are conducive to assessing crop damage and disaster situations in a timely manner by the state and competent departments, and these results have great significance for follow-up disaster relief and macro control.

In addition, measured taken to monitor the freezing injuries of crops should start with studying the crop to strengthen the understanding of the target crop's response when a freezing injury occurs; then, the crop can be monitored in combination with RS techniques. After freezing, the potassium and copper contents in winter wheat have been found to decrease significantly, leading to further changes in the physiological structures of crops (Lacoste *et al.*, 2015). These physiological changes lead to obvious changes in the spectral response of winter wheat. In addition, freezing can also increase the impacts of winter wheat diseases and insect pests. Some studies have shown that frostbite increases the susceptibility of winter wheat to beetles (Lacoste *et al.*, 2015), and various disasters often occur throughout the winter wheat growth season. Using

Advanced Very-High-Resolution Radiometer (AVHRR), LST vegetation index data and satellite-derived RS data can capture important topographic features of freeze occurrences, including changes in latitude, longitude, altitude and distance (Tait and Zheng, 2003). Moreover, the MODIS LST product from the Aqua satellite has been shown to be well-correlated with the minimum air temperature on homogeneous surfaces (Zeng *et al.*, 2015), with increasing variances at high elevations (Pepin *et al.*, 2016). Analyses of ground-based station data have revealed a strong relationship between the freezing intensity and terrain form (Lindkvist *et al.*, 2000). Therefore, it is necessary to monitor and analyse freezing damage using space-based and ground-based RS methods.

Change vector analyses are often used to dynamically monitor land use and coverage; this method is rarely seen in studies monitoring winter wheat freezing injury, and the optimal criteria with which to classify freezing injuries are not yet clear. In this study, CVA was used to dynamically monitor winter wheat land use and coverage and to study the growth recovery of winter wheat following a freezing injury. This method is rarely applied in winter wheat freezing injury monitoring studies, and the reunification

index used herein was the normalized vegetation index, which was also verified by Feng *et al.* (2009) using multitemporal MODIS data to monitor winter wheat freezing injuries. In the study of Wang *et al.* (2011) on the classification of winter wheat freezing injuries based on a CVA method, SIPI was used to characterize the degrees of freezing injury and growth recovery following a freezing injury. The reasons for the differences in their results may involve environmental conditions such as planting, management, water and fertilizer ratio, wheat varieties, sowing date (Yang *et al.*, 2011), terrain (Lindkvist *et al.*, 2000), slope, slope aspect (Xie and Chen, 2008) and other disaster damage conditions. Therefore, the change in the vector angle constructed by the vegetation index cannot be used to completely determine the winter wheat freezing injury and recovery levels.

The geostatistical analysis conducted herein was based on obtaining predictions from a large number of samples by analysing the relationships among the samples and exploring their distribution. In general, the more sample points there are and the gentler the terrain is, the more accurate the forecast results are. However, in this experiment, the terrain conditions were not considered, and the spatial interpolation constraints largely affected the distribution of the results, so there was little deviation between the predicted results and the actual situation. In future studies, we must consider the factors that affect the forecast results to obtain the best possible prediction results.

The growth and development of crops involve all kinds of changes in different environmental factors, characterized by temporal and spatial changes with strong temporal and spatial effects. With the passage of time, the environment and crops are changing, indicating that the factors influencing crop changes are not necessarily the same among different time periods and that the same factors can differently influence winter wheat in different stages. As freezing damage is a natural disaster with a high probability, the methods used to monitor winter wheat freezing injuries must consider the environment at a certain time during the winter wheat freezing injury period, the various factors affecting the normal growth and development of winter wheat at different times, and the resistance of winter wheat under freezing injury stress. Through the combination of these considerations, we can establish a more accurate monitoring mechanism and perform better crop growth monitoring.

## Conclusion

In this study, the map obtained using a CVA and a single vegetation index to analyse the degree of freezing damage shows that the degrees of freezing damage indicated by these methods are roughly the same, but the areas are different; when considering the recovery degree of winter wheat following freezing damage, a difference not only in area but also in location information can be seen. Therefore, a comprehensive analysis method was used to obtain the final winter wheat freezing injury information. Through a comparative analysis of the relationships among the yield, degree of freezing injury and degree of recovery, the combination of the degree of freezing injury and degree of recovery was finally found to have the best yield prediction effect. Therefore, it was best to combine the degree of freezing damage and the degree of recovery to predict the yield range of winter wheat, so as to verify the freezing damage classification accuracy.

**Financial support.** This work was supported by the National Natural Science Foundation of China (31871571, 31201168), Basic Research Program

of Shanxi Province (20210302123411), Outstanding Doctor Funding Award of Shanxi Province (SXYBKY2018040), Key Technologies R&D Program of Shanxi Province (201903D211002-01, 05), Applied Basic Research Project of Shanxi Province (201801D221299), Science and Technology Innovation Fund Project of Shanxi Agricultural University (2020BQ32).

**Conflict of interest.** None.

**Ethical standards.** Not applicable.

## References

- Anderson LG, Hanson DJ and Haas HR (1993) Evaluating land sat thematic mapper derived vegetation indices for estimating above-ground biomass on semiarid rangelands. *Elsevier* **45**, 165–175. [http://dx.doi.org/10.1016/0034-4257\(93\)90040-5](http://dx.doi.org/10.1016/0034-4257(93)90040-5).
- Bascietto M, Cinti BD, Matteucci G and Cescatti A (2012) Biometric assessment of aboveground carbon pools and fluxes in three European forests by Randomized Branch Sampling. *Forest Ecology & Management* **267**, 172–181.
- Cao G, Zhao Y, Duan X and Cao X (2018) Spatial distribution of throughfall of evergreen broad-leaved forest in Mopan Mountain based on Kriging interpolation method. *Journal of Northwest Forestry University* **33**, 19–25.
- Chen C (2012) *Resampling Method in Geometric Correction*. University of Electronic Science and Technology. <http://dx.doi.org/10.7666/d.D763938>.
- Crimp SJ, Zheng BY, Khimashia N, Gobbett DL and Nicholls N (2016) Recent changes in southern Australian frost occurrence: implications for wheat production risk. *Crop and Pasture Science* **67**, 801–811.
- Cuomo V, Lanfredi M, Lasaponara R, Macchiato MF and Simoniello T (2001) Detection of interannual variation of vegetation in middle and southern Italy during 1985–1999 with 1 Km NOAA AVHRR NDVI data. *Journal of Geophysical Research* **106**, 17863–17876.
- Dong YS, Chen HP, Wang HF, Gu XH and Wang JH (2012) Evaluation of winter wheat freezing injury based on multi temporal environmental disaster reduction satellite data. *Journal of Agricultural Engineering* **28**, 172–179.
- Feng MC and Yang WD (2010) Extraction of winter wheat planting area based on RS and selection of the best time phase. *Journal of Shanxi Agricultural University (Natural Science Edition)* **30**, 487–490.
- Feng MC, Yang WD, Cao LL and Ding GW (2009) Monitoring winter wheat freeze injury using multi-temporal MODIS data. *Agricultural Sciences in China* **8**, 1053–1062.
- Frederiks TM, Christopher JT, Sutherland MW and Borrell AK (2015) Post-head-emergence frost in wheat and barley: defining the problem, assessing the damage, and identifying resistance. *Journal of Experimental Botany* **66**, 3487–3498. <http://dx.doi.org/10.1093/jxb/erv088>.
- Gitelson AA, Kaufman YJ and Merzlyak MN (1996) Use of a green channel in remote sensing of global vegetation from EOS-MODIS. *Remote Sensing of Environment* **58**, 289–298.
- Gupta RK, Prasad S, Sessa Sai MVR and Viswanadham TS (1997) The estimation of surface temperature over an agricultural area in the state of Haryana and Panjab, India, and its relationship with the Normalized Difference Vegetation Index (NDVI), using NOAA-AVHRR data. *International Journal of Remote Sensing* **18**, 3729–3741.
- Huang J, Wang A and Zhai S (2015) Spatial interpolation of negative skew distribution data based on Kriging method. *Surveying and Mapping Engineering* **24**, 16–19.
- Jurgens C (1997) The modified normalized difference vegetation index (mNDVI) a new index to determine frost damages in agriculture based on Landsat TM data. *International Journal of Remote Sensing* **18**, 3583–3594.
- Kerdiles H, Grondona M, Rodriguez R and Seguin B (1996) Frost mapping using NOAA AVHRR data in the Pompeian region, Argentina. *Agricultural & Forest Meteorology* **79**, 157–182.
- Kuang ZM, Li Q, Yao YM and Ding MH (2009) Application of EOS/MODIS data in monitoring and evaluation of sugarcane cold damage. *Journal of Applied Meteorology* **20**, 360–364.
- Lacoste C, Nansen C, Thompson S, Moir-Barnetson L, Mian A, Mcnee M and Flower KC (2015) Increased susceptibility to aphids of flowering wheat plants exposed to low temperatures. *Environmental Entomology* **44**, 610–618.

- Lanfredi M** (2003) Multiresolution spatial characterization of land degradation phenomena in southern Italy from 1985 to 1999 using NOAA-AVHRR NDVI data. *Geophysical Research Letters* **30**, 1069–1069.
- Lindkvist L, Gustavsson T and Bogren J** (2000) A frost assessment method for mountainous areas. *Agricultural & Forest Meteorology* **102**, 51–67.
- Liu HQ and Huete A** (1995) A feedback-based modification of the NDVI to minimize canopy background and atmospheric noise. *IEEE Transactions on Geoscience & Remote Sensing* **33**, 457–465.
- Myneni RB and Williams DL** (1994) On the relationship between FAPAR and NDVI. *Remote Sensing of Environment* **49**, 200–211.
- Penuelas J, Baret F and Filella I** (1995) Semi-empirical indices to assess carotenoids/chlorophyll-a ratio from leaf spectral reflectance. *Photosynthetic* **31**, 221–230.
- Pepin NC, Maeda EE and Williams R** (2016) Use of remotely-sensed land surface temperature as a proxy for air temperatures at high elevations: findings from a 5000-meter elevational transect across Kilimanjaro. *Journal of Geophysical Research Atmospheres* **121**, 9998–10015.
- Ren P, Feng MC, Yang WD, Wang C, Liu TT and Wang HQ** (2014) Response of winter wheat (*Triticum aestivum* L.) hyperspectral characteristics to low temperature stress. *Spectroscopy & Spectral Analysis* **34**, 2490–2494.
- Richardson AJ and Wiegand CL** (1977) Distinguishing vegetation from soil background information. *Photogrammetric Engineering and Remote Sensing* **43**, 1541–1552.
- Rouse JW, Haas RW, Schell JA and Deering DW** (1974) *Monitoring the Vernal Advancement and Retrogradation (Green Wave Effect) of Natural Vegetation*. Greenbelt, MD: NASA/GSFC Type III, Final Report. Nasa/gsfct Type Final Report. Available at <https://ntrs.nasa.gov/archive/nasa/casi.ntrs.nasa.gov/19730009608.pdf>.
- Sun PJ, Yang JW, Zhang JS, Pan YJ and Yun Y** (2015) Remote Sensing Extraction of autumn crops based on pattern and change vector analysis. *Journal of Beijing Normal University (Natural Science Edition)* **51**, 89–94.
- Tait A and Zheng XG** (2003) Mapping frost occurrence using satellite data. *Journal of Applied Meteorology* **42**, 193–203.
- Tan ZK, Ding MH, Wang LH, Xin Y and Ou ZR** (2008) Monitoring freeze injury and evaluating losing to sugar-cane using RS and GPS. *Computer and Computing Technologies in Agriculture II* **293**, 307–316.
- Wang CY, Wang SL, Huo ZG, Guo JP and Li J** (2005) Research progress in monitoring, early warning and assessment of Major Agrometeorological Disasters in China in the past 10 years. *Journal of Meteorology* **63**, 121–133.
- Wang HF, Gu XH, Dong YY, Wang JH, Huang WJ, Guo W, Wang DC and Wang K** (2011) Vector analysis of winter wheat freezing disaster and its growth recovery. *Journal of Agricultural Engineering* **27**, 154–159.
- Wang HF, Gu XH, Wang JH and Dong YY** (2012) Monitoring winter wheat freeze injury based on multi-temporal data. *Intelligent Automation & Soft Computing* **18**, 1035–1042. <http://dx.doi.org/10.1080/10798587.2008.10643308>.
- Wang HF, Guo W, Wang JH, Huang WJ, Gu XH, Dong YY and Xu XG** (2013). *Journal of Integrative Agriculture* **12**, 1162–1172. [http://dx.doi.org/10.1016/S2095-3119\(13\)60445-1](http://dx.doi.org/10.1016/S2095-3119(13)60445-1).
- Wang HF, Wang JH, Dong YY, Gu XH and Huo ZG** (2014) Hyperspectral analysis of winter wheat freezing stress and inversion of freezing severity. *Spectroscopy and Spectral Analysis* **34**, 1357–1361.
- Xie X and Chen XY** (2008) An analysis on the freezing damage caused by the low temperature in Hejing in winter, 2006. *Xinjiang Agricultural Sciences* **45**, 269–270.
- Yang BJ, Wang MX and Pei ZY** (2002) Remote sensing monitoring of winter wheat freezing injury. *Journal of Agricultural Engineering* **18**, 136–140.
- Yang JH, Wei JU and Yang XJ** (2011) Cause of freeze injury, cold resistance mechanism and countermeasures of winter wheat. *Journal of Hebei Agricultural Sciences* **15**, 33–36+40.
- Zeng LL, Wardlow B, Tadesse T, Shan J, Hayes M, Li D and Xiang DX** (2015) Estimation of daily air temperature based on MODIS land surface temperature products over the corn belt in the US. *Remote Sensing* **7**, 951–970. <http://dx.doi.org/10.3390/rs70100951>.
- Zhao LC, Li QZ, Zhang Y, Wang HY and Du X** (2020) Normalized NDVI valley area index (NNVAI)-based framework for quantitative and timely monitoring of winter wheat frost damage on the Huang-Huai-Hai Plain, China. *Agriculture Ecosystems & Environment* **292**, 106793.
- Zhu RJ** (2017) *Remote Sensing Monitoring of Wheat Total Erosion Based on Change Vector Analysis*. Henan Agricultural University. <http://cdmd.cnki.com.cn/Article/CDMD-10466-1017281251.htm>.